Scientific Research

Construction and Design of a Cable-Stayed Bridge with Concrete-Filled Steel Tube as a Main Girder

Bo Tian, Ge Wang *, Kai Wen and Ting Zhou

Sichuan Highway Planning, Survey, Design and Research Institute Ltd., Chengdu 610041, China;
* Correspondence: 3867641760@qq.com

Abstract: Herein, a main girder structure for a cable-stayed bridge with concrete-filled steel tubes serving as the main longitudinal ribs is proposed. The feasibility of this structure is verified by calculation and analysis. Then, economic analysis of this structure compared with other types of cable-stayed bridges with main girder structures of the same kind of span is carried out. The results show that the structure is feasible and economical, and it has superior seismic performance, especially in high-intensity and complex mountainous terrain regions in western China.

Keywords: cable-stayed bridge; composite structure; concrete-filled steel tube; cable-girder anchorage; shear lag; initial stress; shear stud; economic index

Citation: Tian, B.; Wang, G.; Wen, K.; Zhou, T. Construction and Design of a Cable-Stayed Bridge with Concrete-Filled Steel Tube as a Main Girder. *Prestress Technology* **2024**, *1*, 27-40. https://doi.org/10.59238/j.pt.2024.01.003

Received: 11/01/2024
Accepted: 17/01/2024
Published: 25/03/2024

Publisher's Note: Prestress technology stays neutral with regard to jurisdictional claims in published maps and institutional affiliations.

1 Introduction

Since the completion of the first modern cable-stayed bridge—the Stroemsund Bridge in Germany—in the 1930s, this type of bridge has been developed rapidly in the past 100 years due to its advantages, such as strong spanning capacity and outstanding wind resistance performance [1] (Table 1). In particular, the completion of a number of world-class bridges, such as the Su-Tong Yangtze River Highway Bridge, the Husutong Yangtze River Bridge, the Stonecutters Bridge in Hong Kong, and the Russky Bridge in Russia, indicates that cable-stayed bridges can be manufactured on the kilometer scale.

The primary factor affecting the span of a cable-stayed bridge is its main girder. The main girder is a member that is subjected to pressure, and it needs to have good compressive strength and a relatively light weight [2,3]. According to incomplete statistics, the main girders of cable-stayed bridges with medium spans (main spans $\leqslant$ 300 m) are mostly used as concrete material due to the great economic advantages of the initial bridge construction investment cost and the subsequent maintenance costs.

However, concrete main girders have some disadvantages. It is difficult for the main span to meet the demand for large spans. As the span increases, the magnitude of increase in the weight of the main girder is greater than that in the material resistance. When the main span exceeds 500 m, the concrete main girder no longer has an advantage. At this time, the structure is prone to cracking, and the durability is poor. Moreover, due to the high weight of the concrete main girder, the cable-stayed bridge with this girder is not conducive to the seismic resistance of bridges.

Composite girders and steel girders solve the span and seismic problems of long-span cable-stayed bridges, but their steel consumption indicators are relatively large, especially for steel box main girders, and their economic performance levels are poor. Improving the durability of concrete main girders, expanding the span range of cable-stayed bridges, and improving the seismic performance of the main bridge are very important research directions.

The unique advantages of concrete-filled steel tubes (CFSTs) are as follows [4]: ① the hoop effect of steel tubes greatly improves the compression capacity of the inner concrete; ② the steel tubes coat the inner concrete, thereby enhancing the cracking resistance of the structure; and ③ under the same bearing capacity, the concrete filled steel tube structure is lighter than others. Engineers have proposed the main girder structure of cable-stayed bridges based on the reinforced concrete-filled steel tube main longitudinal girder (Figure 1).

Table 1 Statistics of cable-stayed bridges with main spans exceeding 300 meters (Unit: m)

No.	Bridge name	Bridge main span	Main girder structural form	No.	Bridge name	Bridge main span	Main girder structural form
1	Russky Bridge, Russia	1104	Steel girder	35	Yanpingba Yangtze River Bridge	480	Hybrid girder
2	Husutong Yangtze River Bridge	1092	Steel truss girder	36	Qingshuipu Bridge	468	Hybrid girder
3	Su-Tong Yangtze River Highway Bridge	1088	Steel girder	37	Fengjie Yangtze River Bridge	460	Concrete main girder
4	Hongkong Stonecutters Bridge	1018	Hybrid girder	38	Yibin Yangtze River Bridge	460	Concrete main girder
5	Qingshan Bridge in Wuhan	938	Hybrid girder	39	Changshou Yangtze River Bridge	460	Concrete main girder
6	E'dong Yangtze River Bridge	926	Hybrid girder	40	Kangjiatuo Yangtze River Bridge in Zhongxian County	460	Concrete main girder
7	Jiayu Yangtze River Highway Bridge	920	Hybrid girder	41	Junshan Yangtze River Bridge	460	Steel beam
8	Jiayu Yangtze Bridge	900	Hybrid beam	42	Hainan Yangpu Bridge	460	Hybrid girder
9	Tatara Bridge, Japan	890	Hybrid girder	43	Shibangou Yangtze River Bridge	450	Concrete main girder
10	Pont de Normandie	856	Hybrid girder	44	Dafosi Yangtze River Bridge in Chongqing	450	Concrete main girder
11	Chizhou Yangtze River Highway Bridge	828	Hybrid girder	45	Hangzhou Bay Bridge North Channel Bridge	448	Steel girder
12	Shishou Yangtze River Bridge	820	Hybrid girder	46	Longxue South Waterway Bridge	448	Hybrid beam
13	Jiujiang Yangtze River Highway Bridge	818	Hybrid girder	47	Lijiatuo Yangtze River Bridge in Chongqing	444	Concrete main girder
14	Wuxue Yangtze River Bridge	808	Hybrid girder	48	Liuhechong Bridge in Bijie	438	Concrete main girder
15	Shanghai Yangtze River Bridge	730	Steel girder	49	Guanyinyan Yangtze River Bridge in Jiangjin	436	Composite girder
16	Shanghai Minpu Bridge	708	Steel truss girder	50	Tongling Yangtze River Highway Bridge	432	Concrete main girder
17	Third Nanjing Yangtze River Bridge	648	Steel girder	51	Kap Shui Mun Bridge in Hongkang	430	Composite girder
18	Second Nanjing Yangtze River Bridge	628	Steel girder	52	Shanghai Nanpu Bridge	423	Composite girder
19	Zhoushan Jintang Bridge	620	Steel girder	53	Shanghai Donghai Bridge	420	Composite girder

No.	Bridge name	Bridge main span	Main girder structural form	No.	Bridge name	Bridge main span	Main girder structural form
20	Baishazhou Yangtze River Bridge	618	Hybrid girder	54	Hejiang Second Yangtze River Bridge	420	Concrete main girder
21	Erqi Yangtze River Bridge	616	Hybrid girder	55	Yunyang Han River Bridge	414	Concrete main girder
22	Yongchuan Yangtze River Bridge in Chongqing	608	Hybrid girder	56	North Branch of Runyang Yangtze River Bridge	406	Steel girder
23	Qingzhou Minjiang Bridge	605	Composite girder	57	Second Wuhan Yangtze River Bridge	400	Concrete main girder
24	Shanghai Yangpu Bridge	602	Composite girder	58	Lidu Yangtze River Bridge in Chongqing	398	Concrete main girder
25	Shanghai Xupu Bridge	590	Hybrid girder	59	Guangdong Panyu Bridge	380	Concrete main girder
26	Taoyaomen Bridge in Zhoushan	580	Hybrid girder	60	Chenzhou Chishi Bridge	380	Concrete main girder
27	Xianyuan Yangtze River Bridge in Nanxi [5]	572	Hybrid girder	61	Wuzuo River Bridge in Bijie	380	Concrete main girder
28	Huangyi Yangtze River Bridge	520	Hybrid girder	62	Huai'an Bridge	370	Concrete main girder
29	Shantou Queshi Bridge	518	Hybrid girder	63	Fourth Ring Hanjiang Bridge in Wuhan	360	Concrete main girder
30	Anqing Yangtze River Highway Bridge	510	Steel girder	64	Hedong Bridge in Guangzhou	360	Hybrid girder
31	Tianxingzhou Yangtze River Bridge in Wuhan	504	Steel truss girder	65	Dongsha Bridge in Guangzhou	338	Hybrid girder
32	Jingzhou Yangtze River Highway Bridge	500	Concrete main girder	66	Xuanji High Speed Rail Shuiyangjiang Bridge	320	Concrete main girder
33	E-Huang Yangtze River Highway Bridge	480	Concrete main girder	67	Heyuan Fengshuba Bridge	320	Concrete main girder
34	Zhanjiang Bay Bridge	480	Hybrid girder	68	Wuhu Yangtze River Bridge	312	Composite main girder

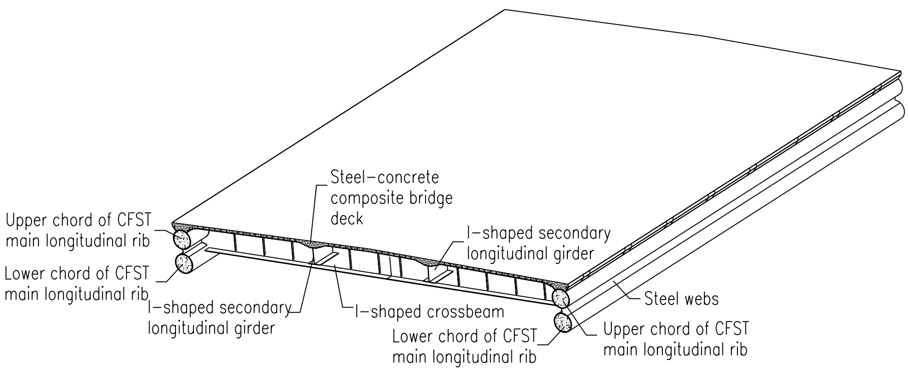

Figure 1 Construction of the main girder with a CFST

The main design concepts of this structure are as follows. ① The main girder adopts a "π" structure with two main longitudinal ribs. The CFST is used as the main longitudinal rib of the beam body to bear most of the axial load. Moreover, anchor structure can also be set on longitudinal ribs. By adjusting the diameter and wall thickness of the steel tube, the grade of internally poured concrete and the number of legs of the steel tubes, the CFST can be applied to different spans. ② In addition, a number of I-beam secondary longitudinal girders are set between two main longitudinal ribs to reduce the lateral span of the bridge deck and the slab shear lag effect. ③ The bridge deck is a steel–concrete composite deck with strip bottom plate and perfobond leiste (PBL) connectors, which transmits part of the axial load and directly bears the wheel load. ④ An I-shaped beam is installed in the direction of the cross bridge between the two main longitudinal ribs.

To date, there are few examples of this type of cable-stayed bridge main girder that have been reported globally. In this paper, a cable-stayed bridge is taken as the research object, and several key constructional parameters and load-bearing characteristics of this type of main girder are investigated for reference.

2 Project Overview

2.1 General Overview

The main span of the cable-stayed bridge with a CFST main girder was 500 m, and it was a three-span cable-stayed bridge with two towers. The side span was 200 m, and the ratio of side-to-mid span was 0.4. An auxiliary pier was arranged at the side span. The cable-stayed bridge adopts a semi-floating structural system. The bridge deck width was based on a two-way four-lane expressway with a designed speed of 80 km/h. The standard subgrade width was 25.5 m, considering 1.2 m wide cable areas on each side of the bridge deck, and the main girder width was 27.9 m.

The bridge towers adopt a steel pipe concrete composite gate-shaped tower. The height of the bridge towers above the bridge deck was 131.0 m, and below the bridge deck was 80.0 m, making the total height of the bridge tower was 211.0 m.

The stay cables were arranged on double-cable planes, and 46 pairs of stay cables were installed on each tower. The standard cable spacing on the main girder was 10.5 m, and the stay cables in the ballast section of the main girder, outside the auxiliary piers of the side spans, were densified to 6.0 m. The cable spacing at the main tower was 2.0 m.

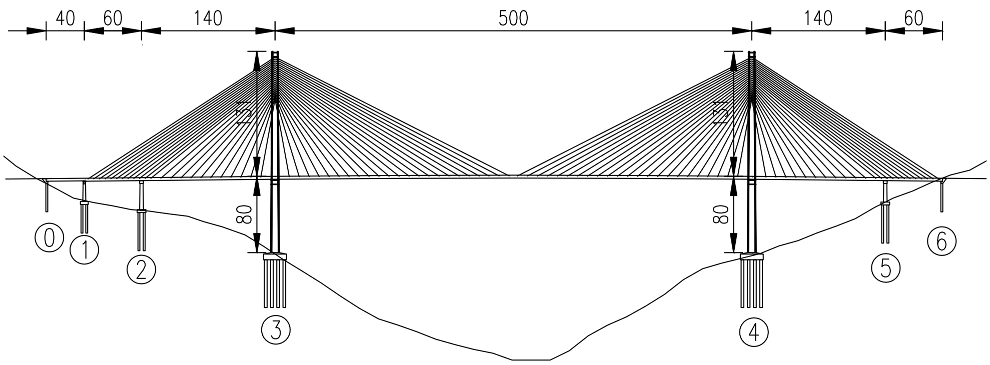

Figure 2 Bridge type layout (Unit:m)

2.2 Design of the Main Girder

The main girder structure featured two longitudinal ribs of concrete-filled steel tube. In addition, the longitudinal rib structure was a dumbbell-shaped double-leg concrete-filled steel tube structure. Considering that the 1.2-m-wide cable areas were on each side of the bridge deck, the width of the main girder was determined to be 27.9 m (Figure 3).

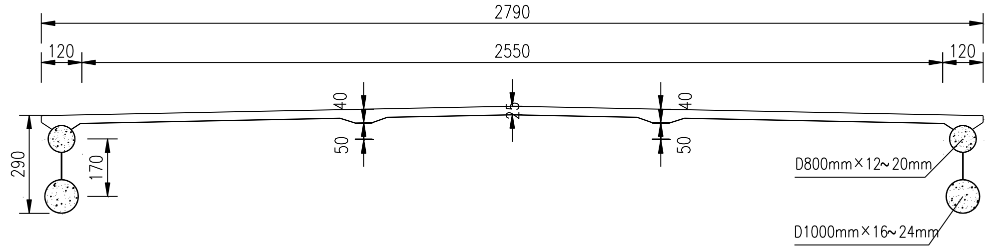

(a) Standard cross section

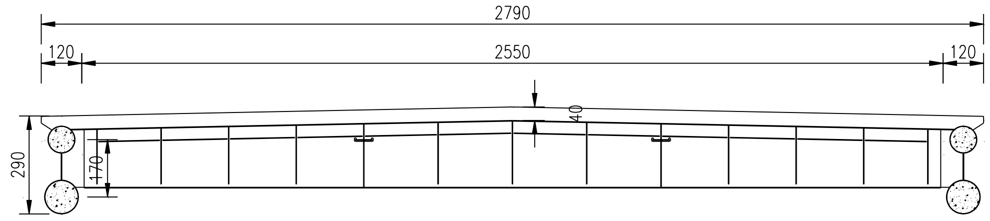

(b) Cross section with the cross beam

Figure 3 Cross section of the main girder (Unit:cm)

The main girder structure was a steel lattice girder consisting of two CFST longitudinal ribs, two small longitudinal girders, and some cross girders. An 8-mm-thick steel bottom plate and PBL connectors were set on the steel lattice girder. Then, a steel fiber-reinforced concrete bridge deck with a standard thickness of 25 cm was poured to form a steel–concrete composite bridge deck.

The double longitudinal ribs of the main girder were composed of a double-tube dumbbell-shaped concrete-filled steel tube structure. The outer diameter of the upper extremity tube was 800 mm, and the outer diameter of the lower extremity tube was 1,000 mm. The two steel tubes were connected by a 20-mm-thick steel plate, and the center-to-center distance between the upper and lower extremity tubes was 1,700 mm. Different wall thicknesses of steel tubes were selected according to the load-bearing conditions at different cross-sectional locations. The thicknesses of the steel tubes for the upper extremities ranged from 12 to 20 mm, and for the lower extremities ranged from 16 to 24 mm. The strength grade of the steel was Q390, and the strength grade of the concrete inside the tube was C60.

The small longitudinal girders were 500-mm-tall I-shaped steel plate girders. The spacing between the girders was 880 cm in the cross-bridge direction, and the distance between the girder and the center of the longitudinal rib was 895 cm.

The steel crossbeam was an I-beam with a height of 2000 mm at the mid-span and a height of 1720 mm at the connection with the longitudinal ribs. Longitudinal and transverse stiffening ribs were placed on the web of the I-beam.

The steel–concrete composite bridge deck was composed of a steel fiber concrete top plate, an 8-mm-thick steel bottom plate, and PBL connectors. The standard thickness of the steel fiber reinforced concrete plate was 25 cm, which was locally thickened to 40 cm at the site of the connection with the steel lattice beam.

The cable-girder anchorage area was composed of an anchor plate, a support plate (stiffened plate), a pressure plate, an end sealing plate, a cable guide tube, and a steel transverse diaphragm inside the tube (Figure 4).

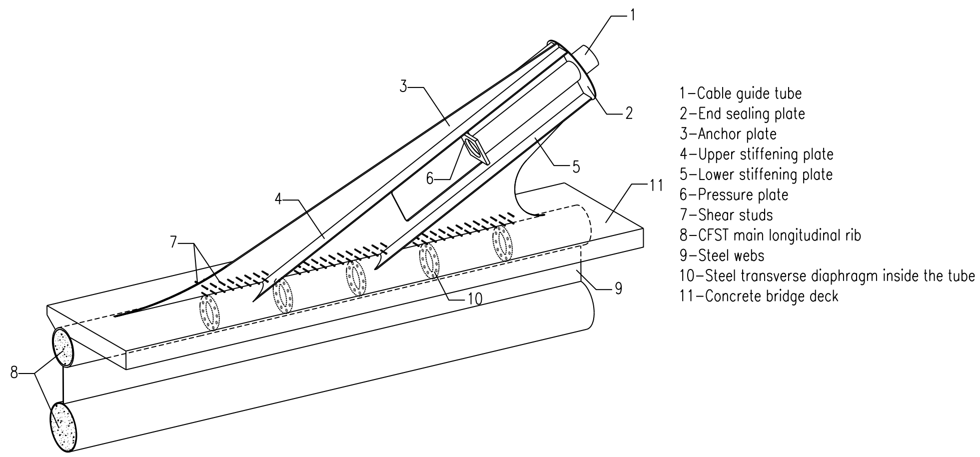

Figure 4 Cable girder anchorage

2.3 Construction of the Main Girder

The core principles of the main girder design of the cable-stayed bridge with the concrete-filled steel tube were to maximize the bearing capacity of the concrete-filled steel tube and to have most of the dead load borne by the main longitudinal ribs of the tube. Based on these concepts, the following construction procedure of the main girder was proposed (Table 2).

Table 2 Construction procedure of the main girder

Step No.	Construction contents
1	Installation of the No. 0 segmental steel structure of the main girder using the bracket or bracket method
2	Symmetric installation of the sections of the main girder from Section 0 to both sides by a deck crane in the maximum cantilever state
3	Pouring of concrete inside the main longitudinal rib steel tubes
4	First cable adjustment
5	Closure mid-span section
6	Symmetric pouring of the bridge deck concrete after the concrete inside the tube reached the design strength starting from block No. 0.
7	Construction of bridge deck ancillary structures
8	Completion of bridge and adjustment of cable

If needed at the end, the steel tubes in the mid-span closure section of the main girder could employ nonconcrete-filled steel tubes.

3 Research Contents and Methods

3.1 Research Contents

According to the characteristics of the main girder of the cable-stayed bridge and the CFST, the main girder is studied from the following aspects in this paper.

(1) Load-bearing capacity of the main longitudinal ribs composed of CFSTs

The main longitudinal ribs composed of steel tubes mainly undergo two states: the maximum cantilever state and the complete state of bridge. In the former state, attention should be given to the maximum stress level of the empty steel tubes. This value is related to the stability in the construction stage and the initial stress of the steel tubes [6]. In the latter state, attention should be given to the internal force of the CFST to ensure that the members are always small eccentric compression members and that the bearing capacity meets the code requirements.

(2) Shear lag effect of the bridge deck

The main girder deck only supports the main longitudinal ribs, and the shear lag effect exists under both the bending moment and axial load [7]. Compared with those of the concrete π-beam, double I-beam, and bilateral steel box composite girder, the width of the CFST main longitudinal rib of the main girder in the cross-bridge direction is smaller. We need to study whether the CFST main longitudinal rib aggravates or reduces the shear lag effect.

(3) Cable-girder anchorage structure

The cable-girder anchorage structure is novel, and the anchor stay plate acts on the radial direction of the steel tube with a line load. Whether the force transfer in the cable-girder anchorage area is smooth and whether there is stress concentration under the action of the stay cable load need to be studied.

(4) Force on the transverse beam

Regardless of whether it has a single-leg arrangement or double-leg dumbbell arrangement, compared with the other main girders, the torsional capacity of the CFST main longitudinal rib is weaker, and the bending moment constraint on the beam ends is smaller. It is necessary to study whether there will be a high stress area at the junction of the longitudinal and transverse beams under the local load of the wheel.

(5) Load-bearing capacity analysis of the steel–concrete joint of main girder

The CFST main girder is composed of CFST main longitudinal ribs, steel I-beam secondary beams, steel I-beams and concrete bridge decks. It is necessary to study whether the steel-concrete connecting pieces connecting the members are stressed reasonably and meet the requirements of the specifications. Moreover, to ensure that the structure meets the plane section assumption.

3.2 Research Methods

In this paper, by means of finite element analysis, three calculation models are established based on the research contents (Figure 5).

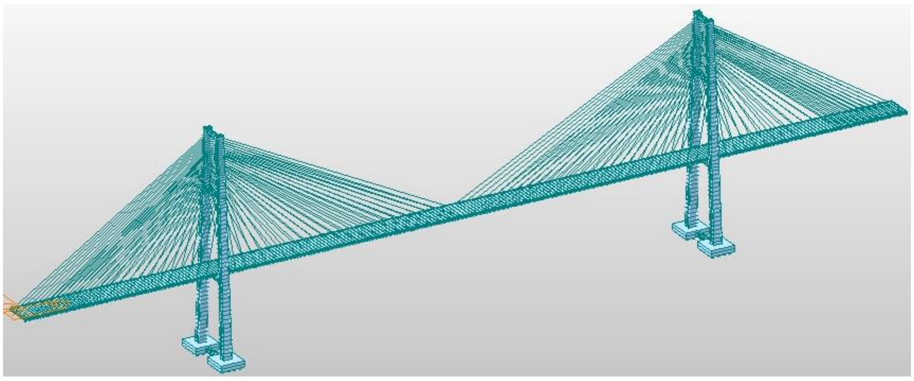

(a) Model 1

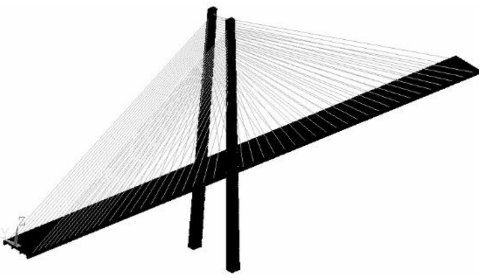

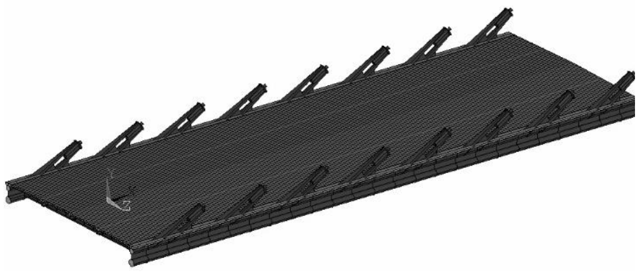

(b) Model 2 (c) Model 3

Figure 5 Finite element models

Model 1 is the overall calculation model. This model is created using Midas software to analyze the structural force during the construction process and the operational state of the full bridge. In the end, a reasonable cable force for the completed bridge was obtained based on the analysis, and the bearing capacity of the main longitudinal rib steel-concrete was verified.

Model 2 represents half of the overall calculation model with an imposed symmetry constraint, and it is created by Ansys software. In the model, the beam-slab mixed element is used for the tower and column, the solid element is used for the concrete main girder, the shell element is used for the steel girder of the main girder, and the truss element is used for the stay cables. This model is mainly used to analyze the shear lag effect of a concrete bridge deck and the load-bearing effect of the beam under the action of wheels.

Model 3 is the local model of the main girder, which uses the main girder segments corresponding to the eight pairs of stay cables with the largest forces and is created using Ansys software. In the model, the cable-girder anchorage construction and the steel–concrete joints [8] are simulated; the concrete is used as a solid element, the steel girder of the main girder is used as a shell element, and the steel–concrete joints are used as three-dimensional virtual spring elements. This model mainly analyzes the force conditions at the cable-girder anchorage area and connector sites.

4 Analysis Results

4.1 Forces on the Main Longitudinal Ribs Composed of CFSTs

In the maximum cantilever state before the concrete is poured into the tube, the vertical load of the main girder is mainly carried by the upper and lower steel tubes of the main longitudinal girder; thus, the axial stiffness of the cross section is relatively small, and the structure is prone to instability. The stability analysis results show that first-order instability is caused by the web connecting the upper and lower tubes. Further comparison shows that adjusting the web thickness can improve the stability (Figure 6). The table shows that as the web thickness increases, the instability factor increases. Therefore, it is recommended that the web thickness be set to 1.5~1.8 times the maximum steel tube wall thickness.

Figure 7 shows the stress conditions of the steel tube at the maximum cantilever stage. The figure shows that the maximum initial stresses of the steel tubes are -68.52 MPa and 56.09 MPa, and the initial stresses of the steel tubes are 0.175 and 0.144, respectively.

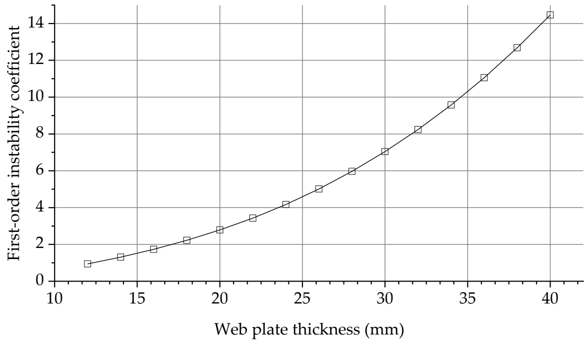

Figure 6 Influence of web thickness on the overall stability

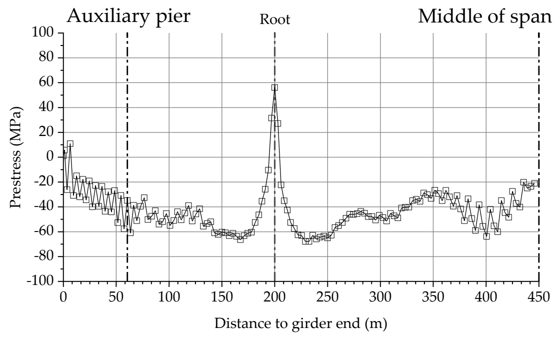

Figure 7 Stress of the main longitudinal rib in the maximum cantilever state before the concrete is poured into the tube

The calculation results show that under the design conditions, the main longitudinal ribs made of concrete-filled steel tubes are small eccentric compression members. According to Article 5.2.2 of the "Specifications for Design of Highway Concrete-filled Steel Tubular Arch Bridges" (JTG/T D65-06—2015), the bearing capacity formula of the eccentric compression members of the concrete-filled steel tube is used for evaluating calculations (Figure 8). The figure shows that the bearing capacity of the main longitudinal ribs made of reinforced concrete-filled steel tubes meets the Specification requirements.

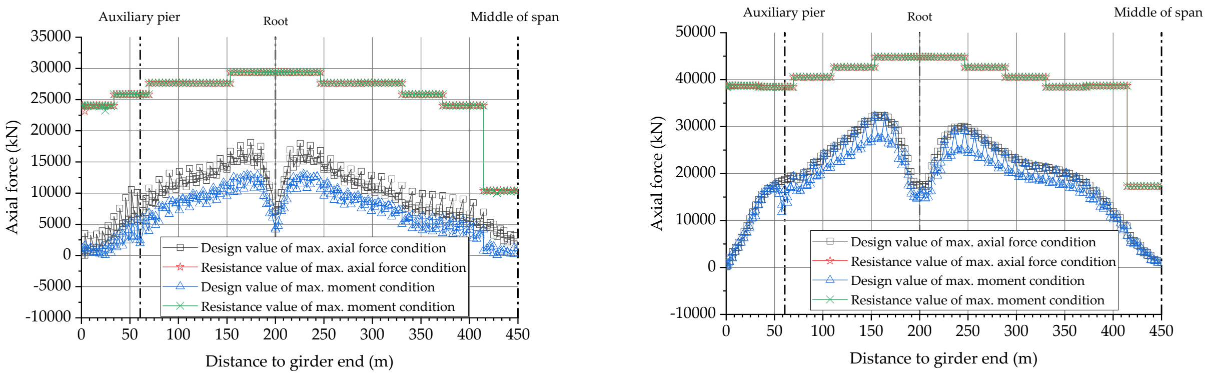

(a) Upper chord of the concrete-filled steel tube (b) Bottom chord of the concrete-filled steel tube

Figure 8 Envelope diagrams of the bearing capacities of the concrete-filled steel tube of the main longitudinal girder

4.2 Forces on the Concrete Bridge Deck

Due to space limitations, only presents the distributions of concrete longitudinal bridge stresses at virous cross-sections of the main girder under dead load conditions (Figure 9). The diagram shows that ① the stress distribution is most inhomogeneous at the roots of the main girder and between the girder end of the side span and the auxiliary pier. This inhomogeneity is manifested as the peak value of the stress near the main longitudinal beam. ② Furthermore, all the cross sections of the remaining locations are basically uniformly stressed.

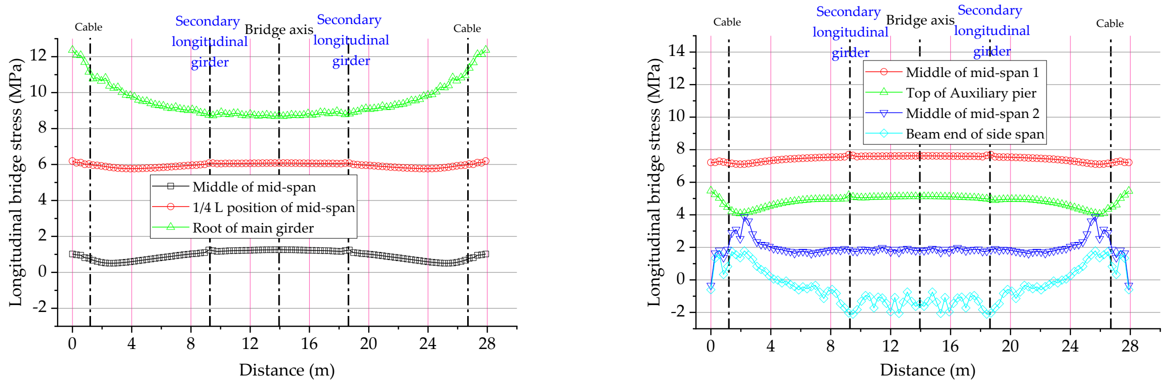

(a) Mid-span of the main beam (b) Side span of the main beam

Figure 9 Stress distribution in the longitudinal bridge direction of the concrete bridge deck slab

According to the definition of the shear lag coefficient, the shear lag coefficient of each cross-section is as follows: 1.293 for the roots of the main girder, 0.934 for the middle of the mid-span, 1.040 for the 1/4 L position of the mid-span, 5.074 for the side span, and 1.985 for the No. 2 section of mid-span of the main girder (between the girder end and auxiliary pier), 1.135 for the auxiliary pier top, 0.916 for the No. 1 section of mid-span of the main girder (between the main girder root and auxiliary pier). A comparison of the shear lag factors at the roots of several other main girders [9-11] (Table 3) shows that the shear lag effect of the main girder with concrete-filled steel tubes and two longitudinal ribs is more obvious than that of the other types of girders.

Table 3 Comparison of the shear lag coefficients of the cross sections of the main girder root for different types of girders

No.	Main girder type	Shear lag coefficient
1	Main girder with two longitudinal ribs composed of concrete-filled steel tubes	1.293

No.	Main girder type	Shear lag coefficient
2	Hedong Yangtze River Bridge, Luzhou city (Double I-beam composite beam)	1.203
3	Wenzhou Dongtou Damen Bridge (Prestressed concrete (PC) π-beam)	1.198
4	Yanpingba Yangtze River Bridge, Yibin city (Steel box composite girder with two sides)	1.081

In this paper, the shear lag effects of the cross sections of main girder roots are compared for steel tubes with different diameters for the main longitudinal girder and with different heights for the secondary longitudinal girders (Figures 10 and 11, respectively). The results indicate that the impact of the above structures on the shear lag coefficient is limited, with a coefficient of 1.290 for a tube diameter of 1.2 m and 1.276 for a secondary girder height of 2.0 m.

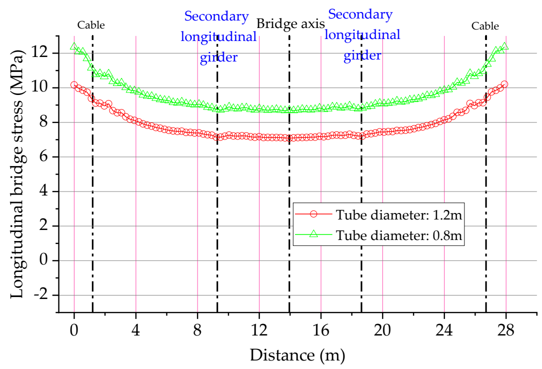

Figure 10 Effect of the steel tube diameter of the main girder on the transverse distribution of stress

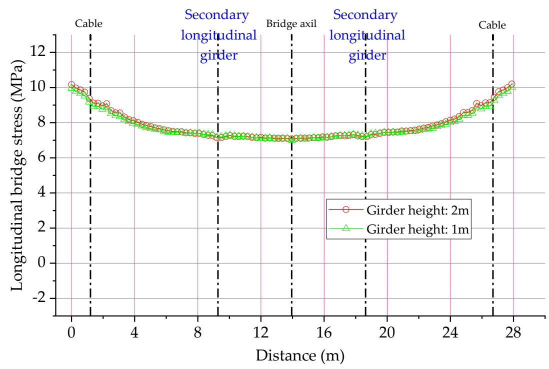

Figure 11 Effect of the height of the secondary longitudinal girder on the transverse stress distribution

4.3 Forces in the Cable-Girder Anchorage Area

Under the maximum cable force, the load-bearing capacity of each plate in the cable-girder anchorage area is shown in the figure. The following information can be observed from the figures:

The overall stress level of the anchor plate is -20~95 MPa, the weld at the connection with the main longitudinal beam steel tube is uniformly stressed, and there is no obvious stress concentration.

The maximum stress in the stiffened slab is approximately 100 MPa. The area with a great stress is located at the pressure-bearing slab toward the bridge tower. The stress level decreases near the main longitudinal ribs.

Under the radial tension, the steel tubes do not exhibit significant stress concentration, indicating that the connection between the anchor plate and the main girder structure is reasonable.

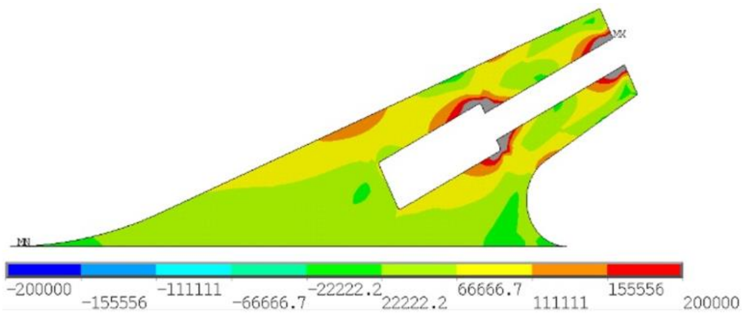

(a) Anchor Plate

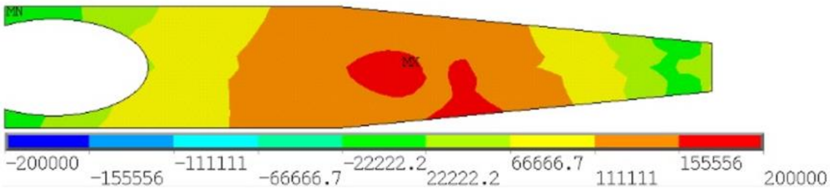

(b) Stiffening plate

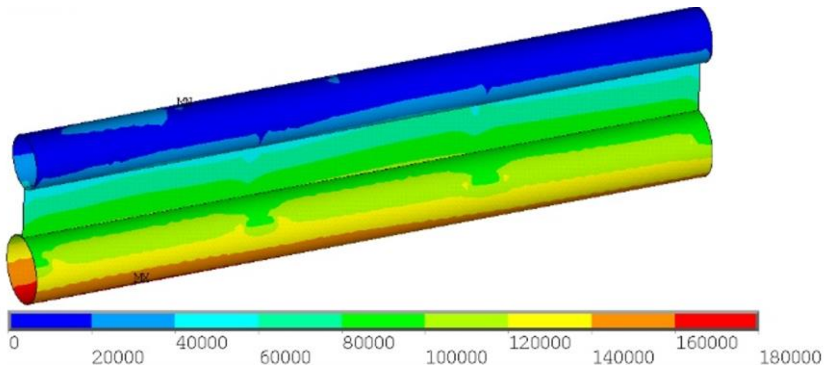

(c) Steel tube and web plate

Figure 12 Von Mises stress of the main plates in the cable-girder anchorage area (Unit: kPa)

4.4 Forces on Steel–Concrete Connectors

The longitudinal shearing forces acting on the shear studs of the main longitudinal girder and the PBL connector of the bridge deck under dead load conditions are calculated and extracted, and the results are shown in the figure.

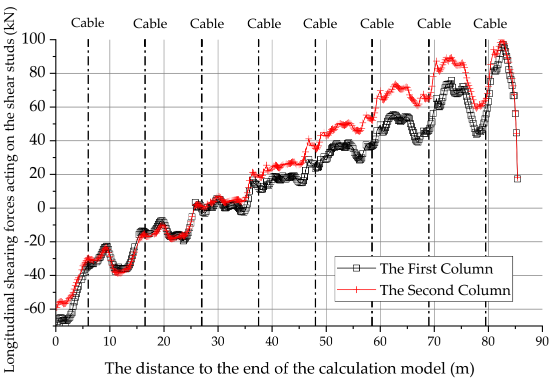

(a) Shear studs of the main longitudinal rib

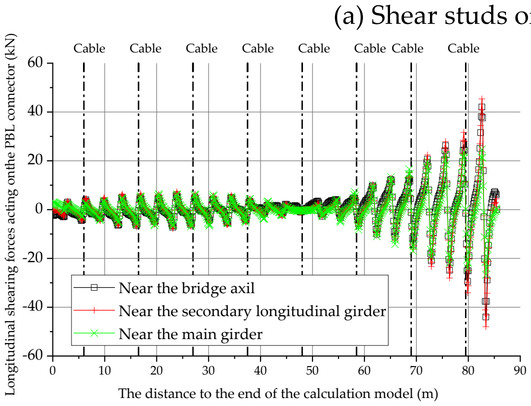

(b) PBL connector on the bridge deck

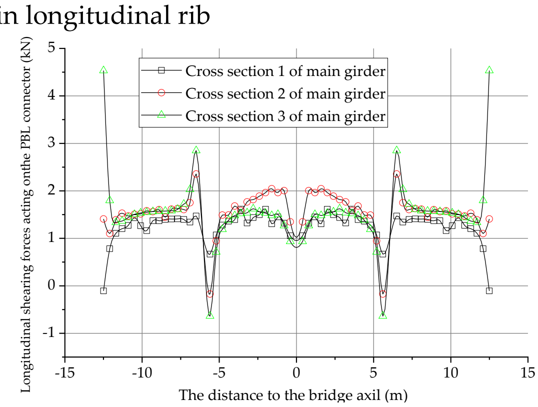

(c) PBL connector on the bridge deck

Figure 13 Longitudinal shear force distribution of the main girder steel–concrete connector

The following information can be obtained from the figure:

(1) The maximum value of the shear studs on the main longitudinal girder is 98 kN, and the maximum value of the PBL connector of the bridge deck is 42 kN. Both of these values meet the specified requirements.
(2) The stress on the shear studs on the main longitudinal girder is significantly greater than that on the PBL connectors in the bridge deck. This difference indicates that the force transfer of the steel structure of the bridge deck and concrete mainly occurs in the main longitudinal ribs. Conversely, the steel bottom plate and the PBL connectors are mainly serve as the bottom formwork for the concrete bridge deck and enhance the load-bearing capacity of the secondary system of the bridge deck respectively.
(3) The stress on the shear studs on the main longitudinal girder in each segment is not uniform, and the stress tends to increase in a step-by-step manner close to the root of the main girder.
(4) The stress on the PBL connector of the bridge deck near the primary and secondary longitudinal girders is significantly greater than that at other locations, indicating that the bridge deck has a shear lag effect.

4.5 Force on the Transverse Beam

By considering Article 4.3.1 of the "Specifications Code for Design of Highway Bridges and Culverts" (JTG D60-2015), we can carry out local loading on the girder. For the calculation, four 550-kN standard vehicles are selected and arranged side by side, with the 140-kN heavy axis wheel loaded directly above the crossbeam.

The calculation results are shown in Figure 14. From the diagram, it can be observed that the stress near the upper chord steel tube on the web of the crossbeam is relatively high, reaching around 200 MPa. This is mainly because the steel tube itself has less torsional stiffness, and at this location, the crossbeam has greater bending stiffness, resulting in a greater distribution of internal forces to the crossbeam. To improve the stress at this location, multiple inclined stiffening ribs are considered along the principal stress direction on the web of the crossbeam. The optimized structural calculation results show that the stress on the web of the crossbeam is significantly improved, with the maximum stress level reduced to around 160 MPa.

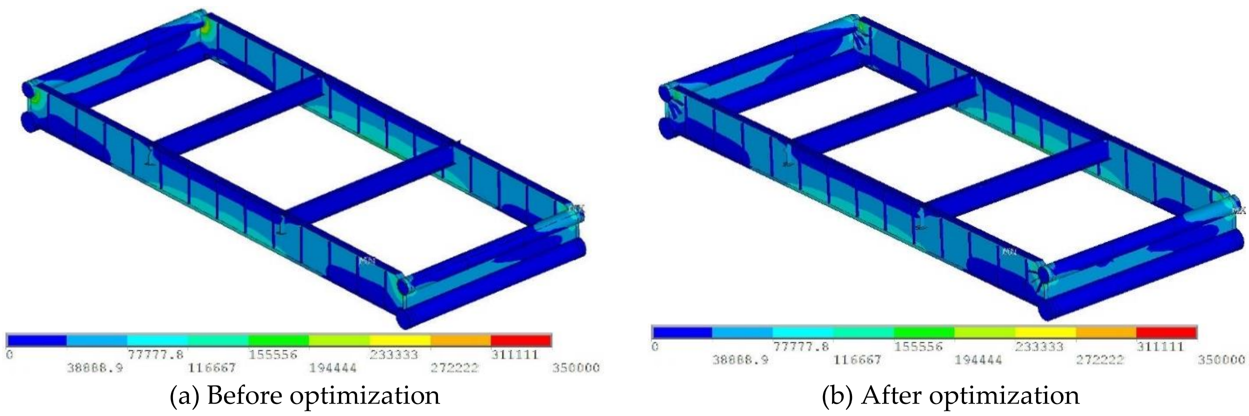

(a) Before optimization (b) After optimization

Figure 14 Von Mises stress contours of the transverse beam (Unit: kPa)

5 Economic Indicators

After clarifying the mechanical characteristics of the CFST main girder, the economic indicators of the 500-meter-span cable-stayed bridges are compared and analyzed (Table 4). The following information can be obtained from the table:

(1) Compared with that of the cable-stayed bridge with a prestressed concrete (PC) girder, the weight of the main girder is reduced by 47.5%~54.8%. Compared with that of the cable-stayed bridge with a steel main girder, the steel usage for the main girder is reduced by 58%.
(2) Compared with that of the cable-stayed bridge with a bilateral steel box composite girder, the weight of the main girder is reduced by approximately 30%.

https://doi.org/10.59238/j.pt.2024.01.003

Compared with that of the cable-stayed bridge with a double I-beam composite girder, the weight of the main girder is basically the same. The overall steel consumption of the main girder is also the same.

(3) After the weight of the main girder is reduced, the numbers of towers, foundations, and stay cables will decrease, and the economic performance will significantly improve.

Table 4 Comparison of the main girder materials and weight indices for cable-stayed bridges with 500-meter main spans

Bridge name	Bridge length	Bridge width	Main girder type	Steel or steel–concrete composite girder segment			Concrete girder segment			Main girder weight
	(m)	(m)		Steel plate (t/m²)	Steel bar (t/m²)	Concrete (m³/m²)	Steel plate (t/m²)	Steel bar (t/m²)	Concrete (m³/m²)	(kN/m²)
CFST Cable-stayed bridge	980	27.9	CFST main girder	0.30	0.08	0.36				13.04
Fengjie Yangtze River Bridge	893	20.5	Double longitudinal rib PC girder				0.12	0.02	0.90	24.95
Yibin Yangtze River Bridge	828	25.0	PK cross-section PC girder				0.24	0.03	1.01	28.89
Changshou Yangtze River Bridge, Chongqing city	874	23.4	Double longitudinal rib PC girder				0.14	0.03	0.89	24.84
Second Hejiang Yangtze River Bridge	840	30.0	Double longitudinal rib PC girder				0.22	0.03	1.01	28.76
Yanpingba Yangtze River Bridge	866	40.0~57.0	Double-sided box hybrid girder	0.27	0.09	0.19	0.20	0.03	1.04	18.51
Huduxi Minjiang River Bridge	840	38.0	Double-sided box hybrid girder	0.35	0.07	0.28	0.23	0.04	1.63	27.80
Lancang River Bridge	700	26.0	Bilateral I-beam Composite hybrid girder	0.29		0.24	0.20	0.05	1.33	22.52
Guanyinyan Yangtze River Bridge	819	36.1	Bilateral I-beam Composite girder	0.37	0.06	0.25				10.82
Junshan Yangtze River Bridge	964	33.8	Steel box girder	0.51						5.07

6 Conclusions

Through constructional design, calculations and analyses on global and local scales, and comparisons and analyses of the economic weight indices of the main girder with concrete-filled steel tubes, the following conclusions can be drawn:

(1) The bridge structure is rationally, and all components meet the specification requirements during construction and during operation.

(2) Overall, this structure exhibits significant economic advantages compared to steel and composite girder cable-stayed bridges and concrete cable-stayed bridges of the same level. Moreover, the structure’s seismic performance improves after its weight is reduced.

(3) There is no need to use formwork when pouring main girder concrete, thus increasing construction efficiency.
(4) This main girder structure is applicable to a wide range of main spans of cable-stayed bridges, with a length of 350~600 m being suitable.

Conflict of Interest: All authors disclosed no relevant relationships.

Data Availability Statement: The data that support the findings of this study are available from the corresponding author, Tian, upon reasonable request.

References

1. Yan, G. *Modern Cable-Stayed Bridge*; Southwest Jiaotong University Press: Chengdu, 1996.
2. Xiang, H. *Conceptual Design of Bridge*; China Communications Press: BeiJing, 2011.
3. Yu, J. The Bridge Type Quadrant Diagram and New Basic Bridge Type: Umbrella Truss Bridge. *Prestress Technology* **2023**, *1*, 15-29, doi:10.59238/j.pt.2023.03.002.
4. Han, L. *Concrete Filled Steel Tubular Structures-Theory and Practice*, 3rd Edition ed.; Science Press: BeiJing, 2016.
5. Tian, B.; Zhou, T.; Wen, K. Study on Key Technology of Assembling Installation of Long-Span Composite Girder Cable-Stayed Bridge. *Prestress Technology* **2023**, *1*, 81-88, doi:10.59238/j.pt.2023.01.007.
6. Zhou, S.; Liu, Q.; Chen, Z. Effect of Initial Stress on Bearing Capacity of Dumbbell Concrete-Filled Steel Tube Arch Bridge. *Engineering Mechanics* **2008**, *25*, 159-165+178.
7. Xu, Z. *Elasticity*, 5th Edition ed.; Higher Education Press: BeiJing, 2016.
8. Liu, Y.; Chen, C.; Zheng, S. Analysis of Force Mechanism of Pylon Anchorage Structure of Fixed-End Steel Anchor Box Type. *Bridge Construction* **2015**, 33-38.
9. Jiang, J.; Ou, Q. Refined Force Analysis of Composite Beam of Long Span Wide Cable-Stayed Bridge. *Municipal Engineering Technology* **2019**, *37*, 72-75,81, doi:10.3969/j.issn.1009-7767.2019.04.025.
10. Ning, B.; Dai, H. Analysis of Shear Lag Effect in Deck Slabs of Cable-Stayed Bridge with Steel Plates and Concrete Slabs Composite Girders. *World Bridges* **2023**, *51*, 82-88, doi:10.20052/j.issn.1671-7767.2023.02.013.
11. Dai, W.; Xiao, W.; Yang, H.; Zhang, S. Shear Lag Effects of Cable-Stayed Bridge with Π-shape Cross-Section Main Girder. *Journal of Transport Information and Safety* **2009**, *27*, 165-168, doi:10.3963/j.ISSN1674-4861.2009.04.039.

AUTHOR BIOGRAPHIES

	**Bo Tian** M.E. Professor Senior Engineer. Graduated from Southwest Jiaotong University. Research Direction: Mainly Research on Bridge Design and Construction Technology. Email: 908585640@qq.com		**Ge Wang** M.E. Senior Engineer. Graduated from Tongji University. Research Direction: Mainly Research on Bridge Design. Email: 3867641760@qq.com
	**Kai Wen** M.E. Senior Engineer. Graduated from Tongji University. Research Direction: Mainly Research on Bridge Design. Email: 444633512@qq.com		**Ting Zhou** M.E. Professor Senior Engineer. Graduated from Southwest Jiaotong University. Research Direction: Mainly Research on Bridge Design. Email: 442577992@qq.com